MAJOR PAPER

Non-physiological Aortic Flow and Aortopathy in Adult Patients with Transposition of the Great Arteries after the Jatene Procedure: A Pilot Study Using Echo Planar 4D Flow MRI

Yumi Shiina[1,2], Kei Inai[1], and Michinobu Nagao[3*]

Purpose: Dilated aortic root and ascending aorta (AAO) with progressive aortic regurgitation is a well-known sequela after arterial switch operation (ASO) in adults with transposition of the great arteries (TGA). We aimed to quantitatively assess aortic flow profiles in adults with TGA after ASO (Jatene procedure with LeCompte maneuver) using echo planar imaging (EPI) 4D flow MRI.

Methods: Prospectively, 9 consecutive adults (30.2 ± 6.6 years) after ASO (Jatene operation with LeCompte technique), 13 consecutive adults (34.3 ± 7.2 years) after the atrial switch operation with Senning procedure, and 8 age-matched control patients, who underwent turbo field echo (TFE) EPI 4D flow MRI (average scan time of approximately 4 min), were enrolled.

Results: TGA after ASO showed a markedly dilated sinus of Valsalva, compared to TGA after atrial switch operation (26.6. ± 4.9 vs. 18.6. ± 1.5 mm/cm^2). Vorticity, helicity, wall share stress (WSS), and energy loss (EL) in the aortic root and the AAO in TGA were greater than in the controls. Vorticity, helicity, WSS, and EL in the aortic root and the AAO were also greater in TGA after ASO than after atrial switch operation. More acute aortic arch angle correlated with greater vorticity of the aortic root, and the significant diameter ratio of the sinus of Valsalva and the AAO was relevant to greater vorticity, helicity, and EL in TGA after ASO.

Conclusion: A non-physiological blood flow pattern of the aortic root was identified in TGA adults after the ASO (Jatene procedure with LeCompte maneuver). Missing spiral looping of the great arteries and the unique structure after the Jatene procedure may play an adjunctive role in promoting aortopathy. The evaluation of aortic flow profile using EPI 4D flow MRI may be useful for risk stratification for aortopathy in this population.

Keywords: *transposition of the great arteries, aortopathy, four-dimensional flow magnetic resonance, echo planar imaging*

Introduction

Transposition of the great arteries (TGA) is a complex congenital heart disease (CHD), in which the two main arteries leaving the heart are reversed (transposed). This condition is also called dextro-transposition of the great arteries (d-TGA). One of the atrial switch operations, the Senning procedure, for TGA was introduced in the late 1950s and had been the preferred surgical approach for TGA until the early 1990s. The Senning procedure involves extensive surgery in the atria, and no prosthetic material is used. A baffle is created within the atria that re-routes the deoxygenated blood coming from the superior and inferior venae cavae to the mitral valve (pulmonary circulation). The anatomic right ventricle (RV) works as the systemic pump (systemic circulation). In other words, ventriculo-arterial mismatch is unrepaired. The novel technique, arterial switch operation (ASO) was developed later and is currently the main operation for TGA. A representative ASO, the Jatene procedure with the LeCompte maneuver, is an anatomic reconstruction at the level of the great arteries with reimplantation of the coronary arteries. The maneuver entails cutting the main pulmonary

[1]Department of Pediatric Cardiology and Adult Congenital Cardiology, Tokyo Women's Medical University, Tokyo, Japan

[2]Cardiovascular Center, St. Luke's International Hospital, Tokyo, Japan

[3]Department of Diagnostic imaging & Nuclear Medicine, Tokyo Women's Medical University, Tokyo, Japan

*Corresponding author: Department of Diagnostic imaging & Nuclear Medicine, Tokyo Women's Medical University, 8-1, Kawadacho, Shinjuku-ku, Tokyo 162-8666, Japan. Phone & Fax: +81-3-3353-8111, Email: nagao.michinobu@twmu.ac.jp
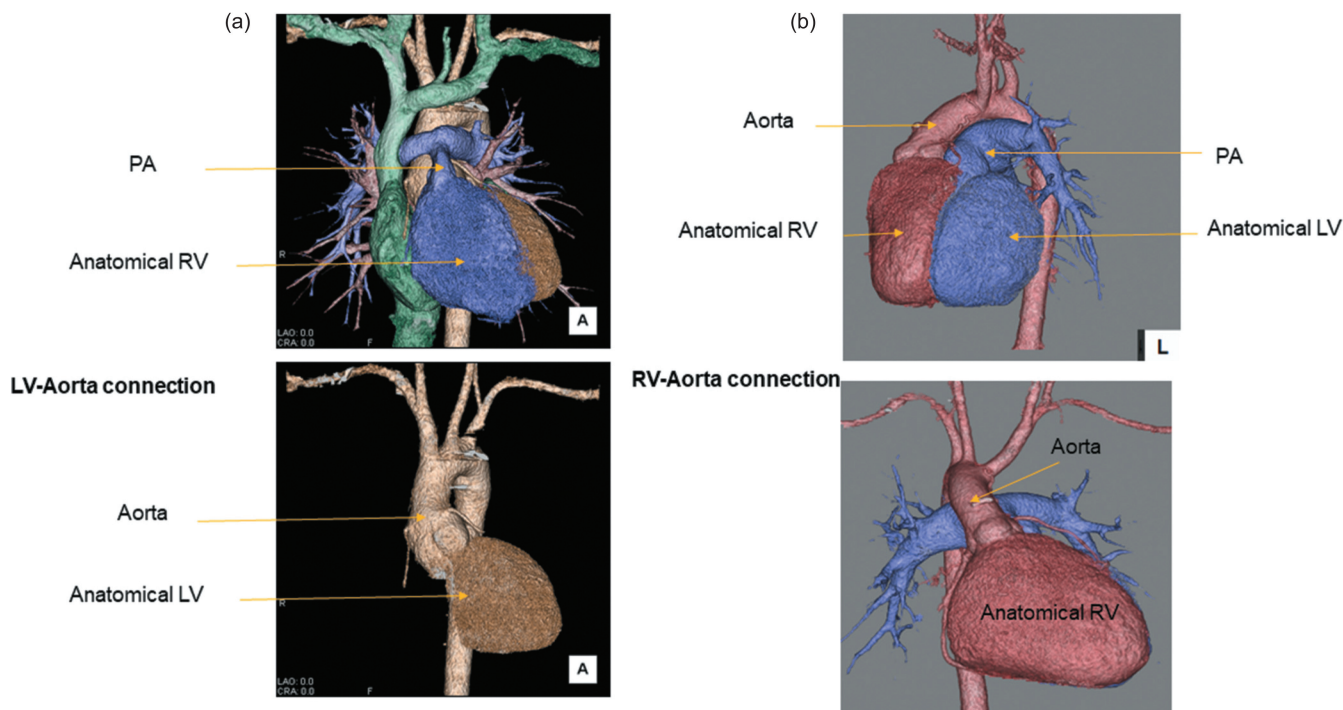
Fig. 1 Images (**a**) of TGA after Jatene procedure with Lecompte maneuver. These images show anatomic reconstruction at the level of the great arteries (LV-aorta connection). The lower image emphasizes the LV-aortic connection. Images (**b**) of TGA after Senning procedure The anatomic RV works as the systemic pump (RV-aorta connection). The lower image emphasizes the systemic RV-aortic connection. LV, left ventricle; RV, right ventricle; TGA, transposition of the great arteries.

artery and moving it anterior to the aorta before reattaching the pulmonary artery; therefore, ventriculo-arterial mismatch is resolved (Fig. 1).

Patients with TGA after ASO show excellent long-term outcomes;[1] however, dilated aortic root and ascending aorta (AAO) with progressive aortic regurgitation is a well-known sequela,[1,2] which sometimes requires surgical intervention. Aortic root dilatation provokes poor cooptation of the trileaflets of the aortic valve, resulting in progressive valve leakage. The etiology of aortic root and/or AAO dilatation, also known as aortopathy, is multifactorial, and the main causes are believed to be congenital histological abnormality, pulmonary arterial banding (PAB), and aortic regurgitation.[1,2]

An abnormal aortic flow profile is also reported in young adolescents with TGA,[3] and hemodynamic abnormalities may be relevant to aortopathy to some extent, but it remains unknown. Healthy adults have a spiral great artery anatomy, with a typical clockwise spiral flow pattern in the aorta,[4] whereas TGA patients after ASO show missing physiological spiral pattern flow in the aorta.[3,5] The main reason for this abnormal flow remains unknown, but may be partially due to unique anatomical structures after ASO (Jatene procedure with LeCompte maneuver) such as acute angulated aortic arch and significant diameter difference between the sinus of Valsalva and the AAO. The cause-and-effect relationship is always challenging to discuss

between abnormal aortic profile and aortopathy; however, it is highly possible that abnormal flow dynamics aggravate aortopathy secondarily. Therefore, it is important to evaluate abnormal aortic flow profiles in high-risk patients with aortopathy.

4D flow MRI enables the quantification of instantaneous viscous energy loss (EL), which is a marker of prominent secondary aortic flow structural abnormality and cardiac workload.[6,7] Elevated EL suggests potential ventriculo-arterial decoupling.

In the present study, we aimed to assess quantitatively aortic flow profiles in TGA adults after ASO (Jatene procedure with LeCompte maneuver) using 4D flow MRI.

Materials and Methods

Nine consecutive patients who underwent ASO (Jatene procedure with LeCompte maneuver) and 13 consecutive patients who underwent the atrial switch operation with Senning procedure, who underwent 4D flow MRI between January 2018 and December 2019, were enrolled. Eight age-matched control patients were also enrolled. These controls underwent MRI for the screening of palpitations and non-specific chest pain. They showed normal results on all tests, including electrocardiography, brain natriuretic peptide (BNP), transthoracic echocardiography, coronary magnetic resonance, computed tomographic angiography, or both.
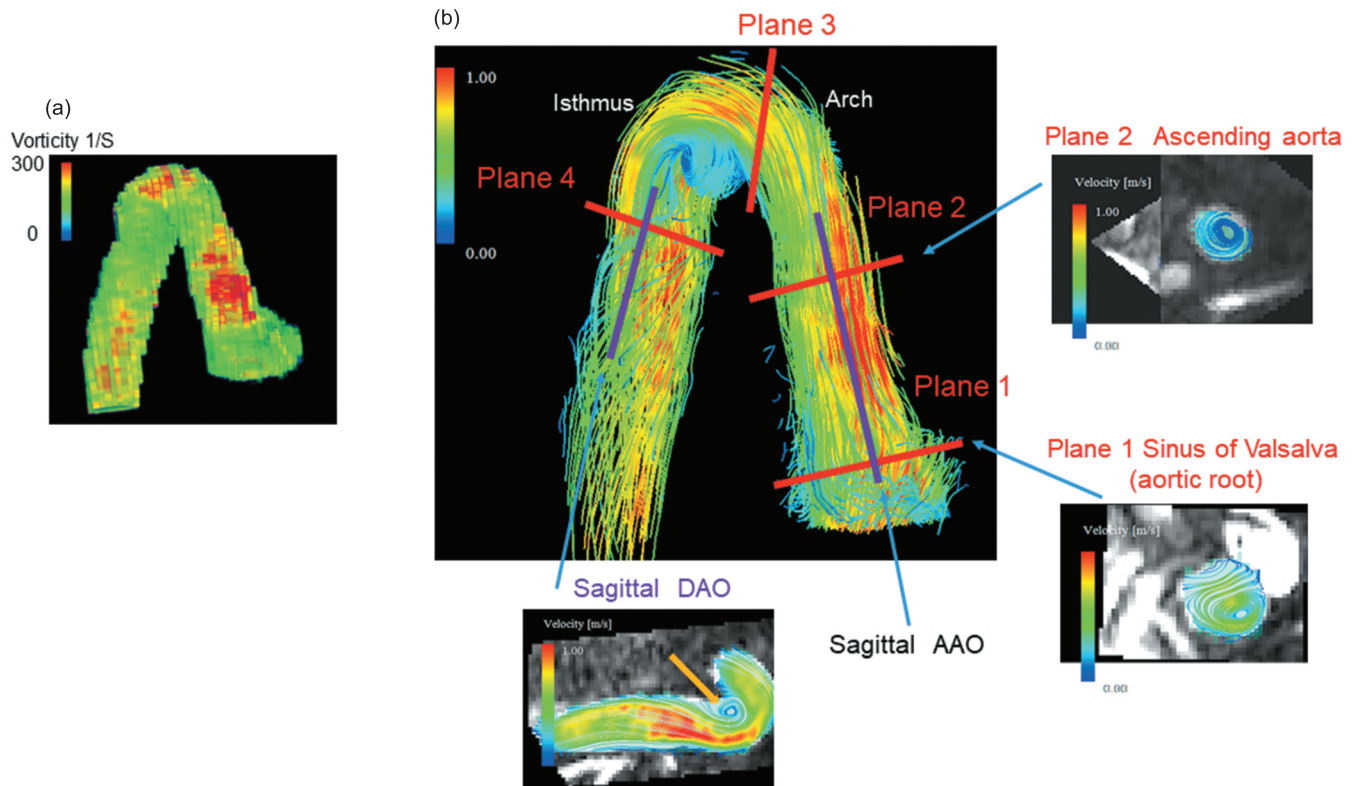
Fig. 2 Measurement sites of the vorticity. **a**: Vorticity map of the ascending, arch, and descending aorta. Vorticity image reconstructed by 3D MRI and red color area shows greater vorticity. **b**: A 3D streamline image of the aorta. We measured vorticities as follows. Plane 1: at the level of the maximum diameter of the sinus of Valsalva, plane 2: mid-AAO at the level of the right pulmonary artery, plane 3: at the arch, and plane 4: at the aortic isthmus (proximal DAO). We also assessed the systolic vorticity of the sagittal plane of the AAO and DAO. The plane 1 image showed greater non-physiological vortex flow of the sinus of Valsalva compared to normal healthy controls. The plane 2 image showed non-physiological vortex flow at the level of mid-AAO. The sagittal image showed greater non-physiological vortex flow of the isthmus (orange arrow). AAO, ascending aorta; DAO, descending aorta.

None of the patients in the control group had hypertension, diabetes mellitus, or ischemic heart disease.

Four Dimensional Magnetic Resonance Imaging

All participants underwent MRI with a 3.0-Tesla whole-body imager (Ingenia 3T Release 5.6; Philips Healthcare, Best, the Netherlands), equipped with a dual-source, parallel RF transmission, and 32-element D torso coil for RF reception. Scan parameters were as follows: FOV, 360 mm; matrix size, 128 × 256; sensitivity encoding (SENSE) factor, 2; EPI factor, 3; TR, 6.2 ms; TE, 3.2 ms; flip angle, 12°; turbo field echo (TFE) factors, 4; actual heart phase, 6.9; temporal resolution, 99 ms; bandwidth, minimum; retrospective trigger, and free breath. Acquisition resolution: 1.97 × 3.28 × 3.00 mm and reconstruction resolution: 1.34 × 1.34 × 1.50 mm.[8–10] The average scan time was approximately 4 min. Contrast medium was not injected. Z-axis field of volume of 140 mm and 93 slices with 3 mm thickness were used.

A flow-sensitive 3D gradient sequence with echo planar imaging (EPI), VENC 150-200 cm/sec, and 14 frames/cycle was used as a 4D flow MRI. 4D flow imaging and calculation of aortic vorticity and helicity were performed using dedicated software for 4D flow MRI (iTFlow; Cardio Flow Design, Tokyo, Japan). Aortic hemodynamics were visualized using time-resolved 3D streamlines, and manually positioned at the level of the sinus of Valsalva, mid-AAO, the arch, and the aortic isthmus level, orthogonal to the aortic lumen. All analysis planes were positioned according to the following anatomical landmarks: plane 1 at the level of the maximum diameter of the sinus of Valsalva, plane 2 mid-AAO at the level of the right pulmonary artery, plane 3 was leveled at the arch, and plane 4 at the aortic isthmus (proximal descending aorta [DAO])(Fig. 2). We also assessed the systolic vorticity of the sagittal plane of the AAO and DAO. Systolic helicity, maximum wall shear stress (WSS), and maximum and averaged viscous EL between the aortic annulus and up to the brachiocephalic trunk were also quantitatively measured (Fig. 3). Vorticity, helicity, WSS, and viscous EL of the area of interest were calculated automatically using the software (Cardio Flow Design) (Fig. 3). Vorticity and helicity
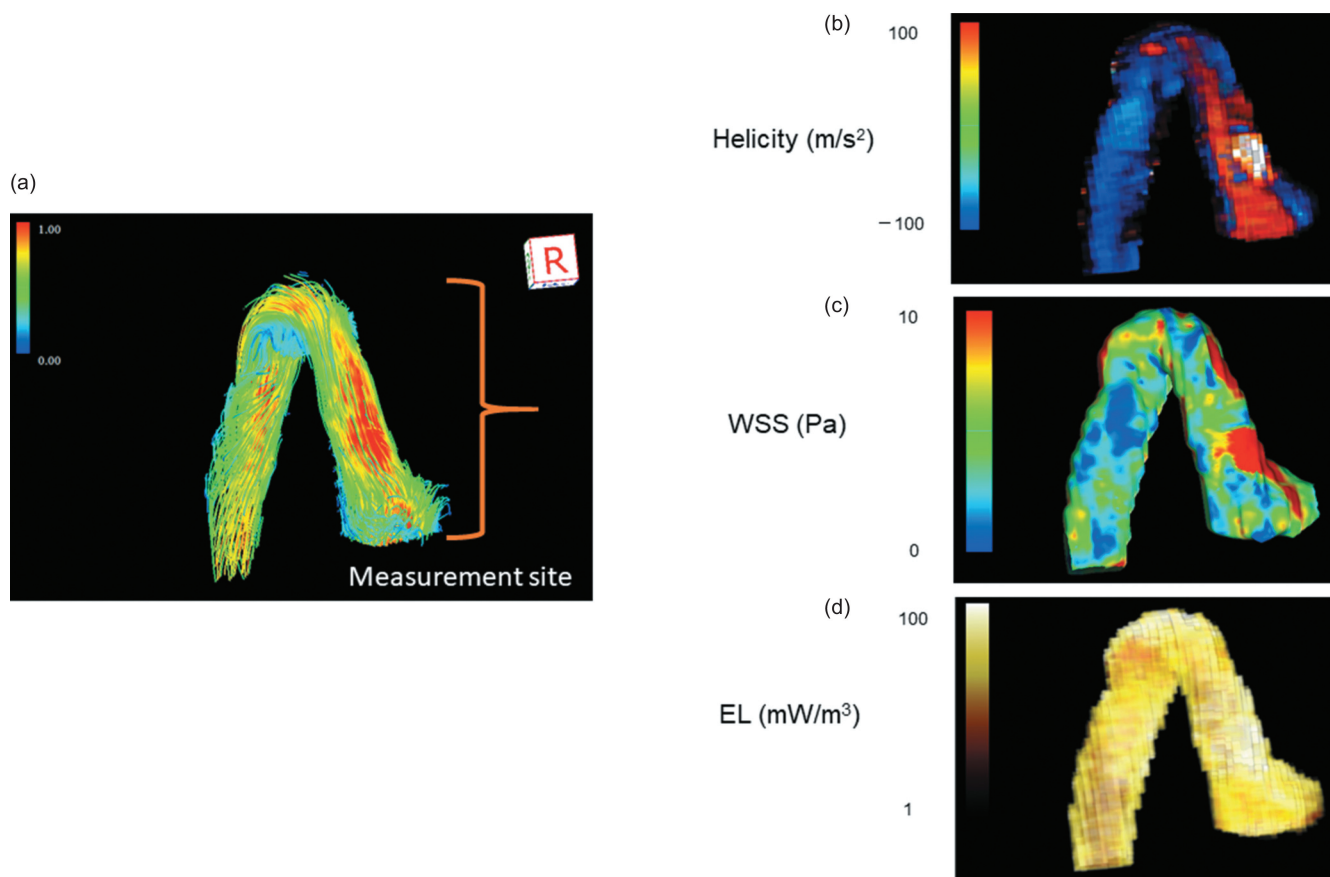
Fig. 3 Measurement site of helicity, WSS, and EL. **a**: 3D streamline image. Systolic helicity, WSS, and EL were measured between the aortic annulus and up to the brachiocephalic trunk. **b**: A helicity image. The red area shows greater clockwise helicity. Greater helicity was identified at the aortic root and AAO in TGA after ASO. **c**: WSS image. The red area shows the maximum WSS, which was identified at the aortic root and AAO in TGA after ASO. **d**: EL image. TGA after ASO showed greater EL compared to healthy controls. AAO, ascending aorta; ASO, arterial switch operation; EL, energy loss; TGA, transposition of the great arteries; WSS, wall share stress.

were analyzed from 4D flow velocity vector fields in each temporal phase, using a bilinear interpolation scheme over the entire anatomical region of interest defined by reconstructed 3D MRI. Vorticity is, in mathematical terms, a vector (the curl of the velocity field describing the local flow rotation rate). Unlike vorticity, helicity is a scalar describing the relationship between flow and propensity toward developing turbulent flow.[11]

Cine imaging with SSFP sequence and 2D phase contrast were scanned before 4D flow MRI. Geometric data for the aortic arch were collected by measuring the following parameter according to Hasegawa's report[12] as shown in Fig. 4: "Arch angle" between the two tangent lines from the highest point of the aortic arch to the centerline of the aortic arch at the level of the brachiocephalic artery, on sagittal oblique images. We also defined sinus of Valsalva-AAO ratio as the diameter of the sinus of Valsalva divided by the diameter of the AAO by measuring the maximum dimensions on 2D images.

Aortic flow patterns by 3D stream lines were viewed dynamically and evaluated by two independent observers (one radiologist with a 20-year experience of cardiac MRI and one adult congenital heart disease specialist with a 10-year experience of cardiac MRI), blinded to the results of the other evaluator. The measurements of both observers were averaged.

The study protocol conformed to the ethical guidelines of the 1975 Declaration of Helsinki. A priori approval was received from the institution's human research committee, and the ethical committee of our hospital approved our study. All patients provided informed consent for undergoing MRI, and written informed consent was obtained from all patients in this study.

Statistical Analysis

All statistical analyses were performed using commercially available software (SPSS 21.0; IBM, Armonk, NY, USA). The Mann–Whitney U-test for independent samples was used to compare the two groups. The Kruskal–Wallis test was applied to compare all three groups at once. Continuous variables were assessed using Pearson's or Spearman's correlation coefficients.
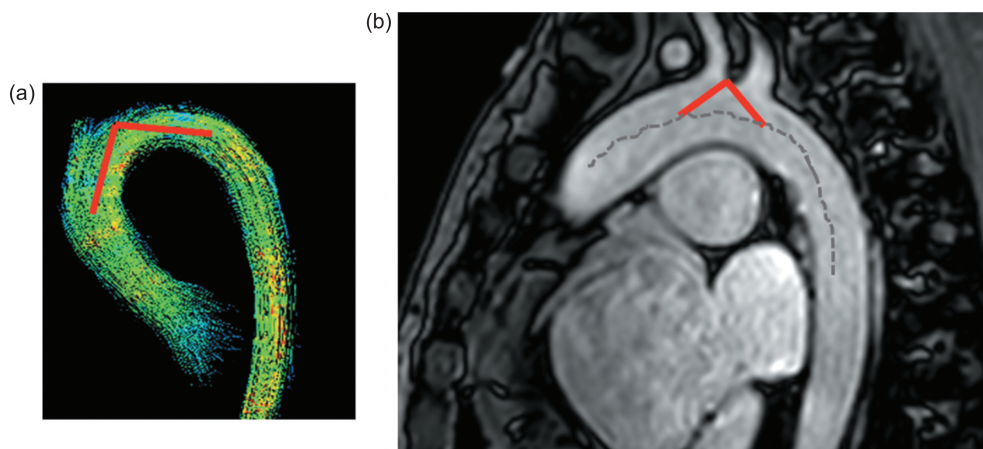
Fig. 4 Measurement of the arch angle (**a**). The arch angle between the two tangent lines from the highest point to the centerline of the aortic arch at the level of the brachiocephalic artery, on sagittal oblique images (**b**).

In order to assess the inter-observer agreement of the vorticity, five randomly selected data were re-analyzed by a second experienced imager who was blinded to patient-identifying data and the first set of measurements. To assess the intra-observer agreement of the vorticity, five randomly selected data were re-analyzed by the first experienced imager after a 2-week interval, blinded to clinical outcomes and the first set of measurements

Results

Patients' characteristics and basic MRI data (Table1)

Patient characteristics are shown in Table 1. A total of nine TGA patients after ASO (Jatene procedure with LeCompte maneuver) (mean age: 30.2 ± 6.6 years), 13 TGA patients after atrial switch operation (Senning procedure) (mean age: $34.3 + \pm 7.2$ years), and 8 age-matched controls were enrolled in the study. There was no significant difference in age, blood pressure between TGA patients, or controls. Seven out of nine patients in the Jatene group underwent PAB before ASO.

The diameter of the sinus of Valsalva was significantly greater in TGA patients after Jatene than in those after Senning ($P < 0.05$) and controls. The diameters of the aortic isthmus were greater in TGA patients after Jatene than after Senning ($P < 0.05$). Compared to controls, TGA patients after Jatene showed smaller AAO, arch, and aortic isthmus. TGA patients after Jatene showed a more acute aortic arch ($109.0 \pm 19.8°$ vs. $146.0 \pm 6.9°$, $P < 0.001$) and greater AR regurgitant fraction ($P = 0.037$) than those after Senning. There was no statistical difference in ejection fraction or cardiac index between TGA patients after Jatene and those after Senning.

Vorticity, helicity, WSS, and viscous EL (Tables 2,3) (Figs. 2,3,5,6)

Compared to age-matched controls, TGA patients after Jatene and those after Senning showed greater vorticity at the level of Valsalva, AAO, arch, aortic isthmus, sagittal AAO, and sagittal DAO. TGA patients after Jatene had greater vorticity at the level of Valsalva, AAO, arch, aortic isthmus, and sagittal AAO than those after atrial switch operation. As for helicity, TGA patients after Jatene and those after Senning showed greater clockwise and counter-clockwise helicities of the AAO and DAO than the controls. TGA patients after Jatene had greater clockwise helicities of the AAO and DAO than those after Senning. There was no significant difference in the counterclock-wise helicities between TGA patients after Jatene and those after Senning.

Maximum WSS, peak EL, and average EL were greater in TGA patients after Jatene and in those after Senning than in controls. TGA patients after Jatene showed greater maximum WSS, peak EL, and average EL than those after Senning.

Correlations with arch angle, aortic root dilatation, and 4D flow parameters (Table 4)

Arch angle negatively correlated with clockwise and counterclockwise vorticities at the level of the sinus of Valsalva (R = - 0.70, - 0.70. $P = 0.037$, 0.036) and aortic isthmus (R = - 0.71, -0.72. $P = 0.032$, 0.028). The arch angle was also negatively correlated with the Valsalva-AAO diameter ratio (R = -0.72, $P = 0.03$).

Valsalva-AAO diameter ratio positively correlated with clockwise and counterclockwise vorticities at the level of the sinus of Valsalva (R = 0.72, 0.72. $P = 0.029$, 0.028). Valsalva-AAO diameter ratio also positively correlated with the clockwise helicity of the AAO. The counterclock-wise helicity of the AAO showed a tendency to correlate with the Valsalva-AAO diameter ratio, which was not statistically different ($P = 0.07$). Peak EL also positively correlated with Valsalva-AAO diameter ratio (R = 0.69, $P = 0.04$).

Table 1 Basic characteristics

	TGA Jatene 9 patients	TGA Senning 13 patients	Controls	3 groups P value	Jatene vs Senning P value
Age (years)	30.2 ± 6.6	34.3 ± 7.2	30.4 ± 8.2	0.21	ns
Duration after surgery (years)	28.1 ± 7.5	27.8 ± 5.9	-	-	ns
AR > 3	1	0	-	-	
Previous PAB	7	-	-		
Age at ICR (month)	7.86 ± 5.6	14.8 ± 14.5	-	-	
Systolic BP (mmHg)	110.0 ± 10.5	108.6 ± 20.3	115.6 ± 14.0	0.68	ns
Diastolic BP (mmHg)	63.8 ± 19.1	65.7 ± 16.2	74.4 ± 6.2	0.47	ns
Sinus of Valsalva (mm/cm^2)	26.6 ± 4.9	18.6 ± 1.5	20.1 ± 1.7	0.005	< 0.05
STJ (mm/cm^2)	15.3 ± 3.6	13.7 ± 1.8	15.9 ± 1.1	0.48	ns
Ascending Ao (mm/cm^2)	14.2 ± 3.5	13.7 ± 1.5	16.5 ± 1.6	0.02	ns
Arch (mm/cm^2)	14.0 ± 2.1	12.2 ± 1.4	16.8 ± 1.5	0.01	ns
Aortic isthmus (mm/cm^2)	14.3 ± 2.4	12.0 ± 1.2	16.7 ± 1.3	0.002	< 0.05
Valsalva-AAO ratio	1.81 ± 0.3	1.37 ± 0.2	1.20 ± 0.2	< 0.001	< 0.05
AR RF (%)	13.0 ± 7.0	4.8 ± 2.2	-	-	< 0.05
Angle (°)	109.0 ± 19.8	146.0 ± 6.9	156.3 ± 8.1	0.003	0.001
EDVI (cc/m^2)	103.0 ± 32.0	110.4 ± 74.6	83.6 ± 12.4	0.43	ns
EF (%)	53.8 ± 9.4	50.6 ± 16.5	61.4 ± 8.2	0.28	ns
CI (cc/min/m^2)	2.91 ± 0.32	2.74 ± 0.26	3.84 ± 0.36	0.005	ns

Ao, aorta; AAO, ascending aorta; AR, aortic regurgitation; BP, blood pressure; CI, cardiac index; EDVI, indexed end-diastolic volume; EF, ejection fraction; ICR, intracardiac repair; ns, not significant; PAB, pulmonary arterial banding; RF, regurgitant fraction; STJ, sino-tubular junction.

Reproducibility

Intra-observer agreement was relatively good for the vorticity (interclass correlation coefficient [ICC]: 0.84, 95%. cardiac index [CI]: 0.56, 0.95). Inter-observer agreement was also relatively good (ICC: 0.75, 95%. CI: 0.38, 0.91).

Discussion

This is the first prospective, single-center study to quantitatively analyze the vorticity and helicity of the aorta in adults with TGA after the Jatene procedure using 4D flow MRI. The novel finding in this study is that adult TGA patients after the Jatene procedure presented with greater non-physiological blood flow profiles in the aorta than those who underwent Senning. Our detailed findings were as follows: 1) vorticity, helicity, WSS, EL in the aortic root, and AAO in TGA patients were greater than those in the controls; 2) vorticity, helicity, WSS, and EL in the aortic root and AAO were greater in TGA patients after Jatene than in those after Senning, and 3) Acute arch angle

and the ratio of the sinus of Valsalva and the AAO were relevant to greater vorticity, helicity, and EL in TGA patients after Jatene.

Aortopathy in TGA

The conventional main reason for aortopathy in TGA is the genuine pulmonary root's different tissue, which expands under systemic pressure conditions, as is seen after Ross operations. Lalezari et al. demonstrated that the neo-aortic root has some histopathological deficiencies in collagen content; therefore, the main reason is considered to be vulnerable neo-aortic root tissue.[13] Additional possible reasons are the influence of PAB, aortic regurgitation, or both.[1,2,14] Aortic flow profiles were also reported to be abnormal, even in children, with only mild valve insufficiency, in particular, the Jatene procedure.[2] Regional abnormal helices or vortices present in 83% of TGA patients after the Jatene procedure with the LeCompte maneuver,[5] and physiological helical flow, which is present in the aorta of healthy individuals, were missing.[3,5] This phenomenon is similar to other

Table 2 Vorticity

	TGA Jatene 9 patients	TGA Senning 13 patients	Controls	3 groups P value	Jatene vs Senning P value
Sinus of Valsalva					
R systolic vorticity (m^2/s)	0.017 ± 0.01	0.0066 ± 0.0014	0.0021 ± 0.0011	0.003	< 0.05
L systolic vorticity (m^2/s)	0.020 ± 0.012	0.0065 ± 0.0007	0.0021 ± 0.0011	0.02	< 0.05
Ascending aorta					
R systolic vorticity (m^2/s)	0.013 ± 0.007	0.0066 ± 0.0045	0.0035 ± 0.0038	0.002	< 0.05
L systolic vorticity (m^2/s)	0.014 ± 0.007	0.0061 ± 0.0009	0.0011 ± 0.0010	0.0007	< 0.05
Arch					
R systolic vorticity (m^2/s)	0.010 ± 0.003	0.0067 ± 0.008	0.0018 ± 0.0014	0.002	< 0.05
L systolic vorticity (m^2/s)	0.010 ± 0.003	0.0076 ± 0.008	0.0016 ± 0.0014	0.003	< 0.05
Aortic isthmus					
R systolic vorticity (m^2/s)	0.017 ± 0.010	0.0067 ± 0.004	0.0016 ± 0.0015	0.002	< 0.05
L systolic vorticity (m^2/s)	0.018 ± 0.012	0.0071 ± 0.005	0.0013 ± 0.0013	0.002	< 0.05
Sagittal AAO systolic vorticity (m^2/s)	0.065 ± 0.02	0.052 ± 0.02	0.0053 ± 0.0017	0.002	< 0.05
Sagittal DAO systolic vorticity (m^2/s)	0.024 ± 0.008	0.023 ± 0.007	0.0050 ± 0.0015	0.006	ns

AAO, ascending aorta; DAO, descending aorta; EL, energy loss; L, counterclockwise; ns, not significant; R, clockwise; TGA, transposition of the great arteries; WSS, wall shear stress.

Table 3 Helicity, WSS, and EL

	TGA Jatene 9 patients	TGA Senning 13 patients	Controls	3 groups P value	Jatene vs Senning P value
Ascending aortic helicity					
R systolic helicity (m^3/s^2)	$7.0 \pm 4.0 \times 10^{-4}$	$5.4 \pm 5.8 \times 10^{-4}$	$1.8 \pm 1.4 \times 10^{-4}$	0.01	< 0.05
L systolic helicity (m^3/s^2)	$7.7 \pm 5.0 \times 10^{-4}$	$7.3 \pm 5.5 \times 10^{-4}$	$1.6 \pm 1.4 \times 10^{-4}$	0.013	ns
Descending aortic helicity					
R systolic helicity (m^3/s^2)	$8.7 \pm 3.0 \times 10^{-4}$	$6.3 \pm 6.7 \times 10^{-4}$	$1.6 \pm 1.3 \times 10^{-4}$	0.005	< 0.05
L systolic helicity (m^3/s^2)	$8.6 \pm 5.0 \times 10^{-4}$	$8.1 \pm 6.8 \times 10^{-4}$	$1.4 \pm 1.1 \times 10^{-4}$	0.012	ns
Ascending aorta					
Maximum WSS (Pa)	26.0 ± 7.7	20.3 ± 6.7	14.8 ± 3.1	0.04	< 0.05
Peak EL (mW/cm3)	0.087 ± 0.046	0.048 ± 0.012	0.029 ± 0.023	0.02	< 0.05
Average EL (mW/cm3)	0.029 ± 0.02	0.012 ± 0.04	0.006 ± 0.006	0.03	< 0.05

EL, energy loss; L, counterclockwise; ns, not significant; R, clockwise; TGA, transposition of the great arteries; WSS, wall shear stress.

aortopathy syndromes such as bicuspid aortic valves (BAV).[15,16] Patients with BAV have histologically vulnerable AAO walls, and their abnormal flow dynamics play an adjunctive role in accelerating aortopathy secondarily.[15] From this perspective, abnormal flow dynamics in patients after the Jatene procedure may also have a secondary negative impact on aortopathy.

Aortic flow profiles in TGA
As for aortic flow dynamics, the physiological spiral stream is well known to be very important.[4] The normal heart has a clockwise spiral pattern of the outflow tracts and of the great arteries.[4] The helical or spiral flow pattern, present in the human aorta in healthy subjects, results, at least partly, from the right-handed twist of the great arteries, curvature of the arch, and pulsatility of flow, which was demonstrated by Kilner.[4] This spiral flow has beneficial effects on cardiac work and on protecting the arterial wall from atherogenesis, as demonstrated in aortic segments of rabbits.[17] Furthermore, swirling flow resulted in reduced uptake of atherogenic low-density lipoproteins by the arterial wall.[17] In TGA patients, this normal spiral structure
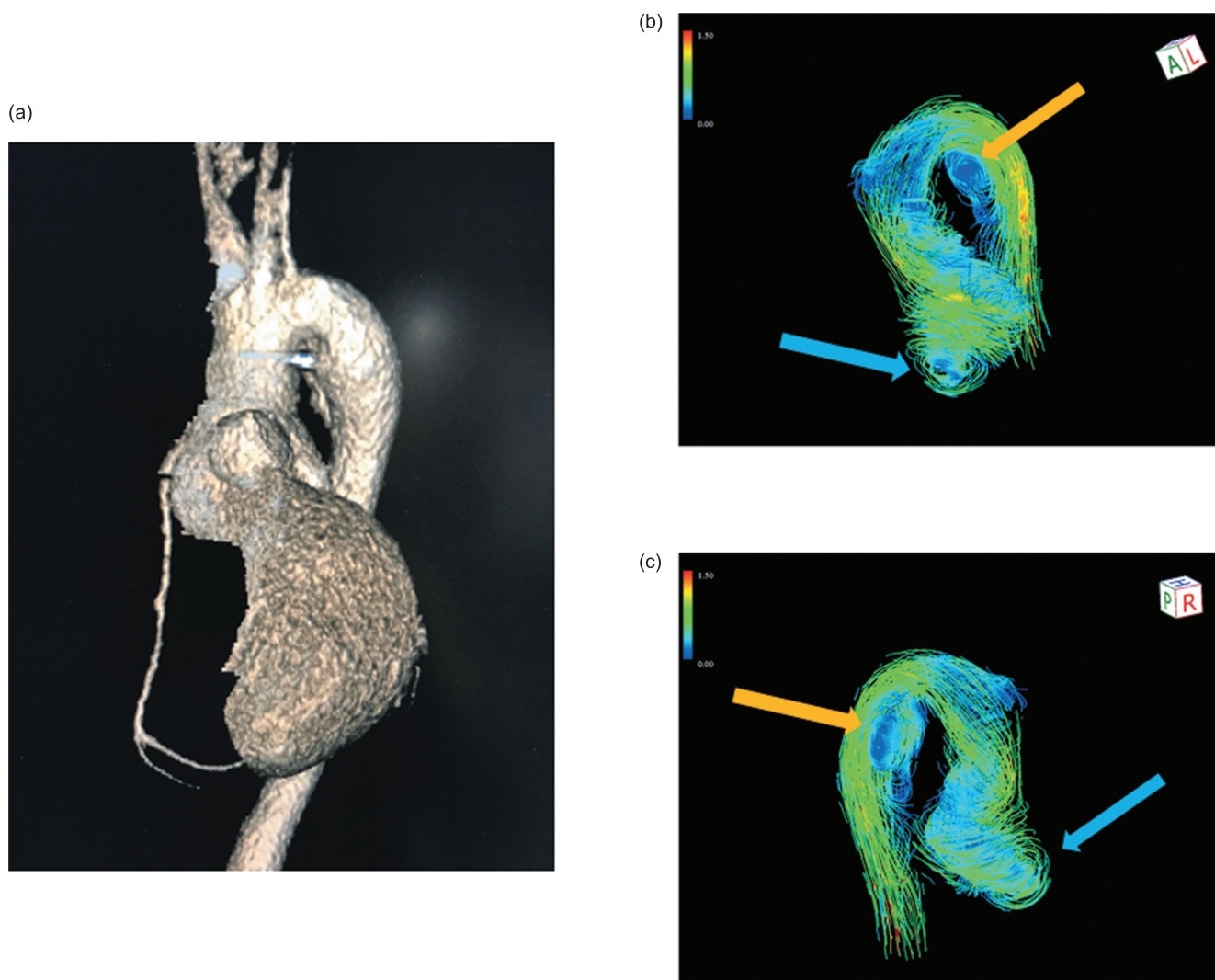
Fig. 5 4D aortic streamline images in TGA after Jatene procedure. A 3D image showed the aorta of a 38-year-old man after the Jatene procedure. He showed an acute aortic arch and a dilated sinus of Valsalva (**a**). A non-physiological, greater vorticity at the level of sinus of Valsalva (blue arrow), and a non-physiological vorticity of the isthmus (orange arrow) were identified (**b** and **c**). TGA, transposition of the great arteries.

pattern is missing as part of the disease, and hence, the missing physiological helicity could partially be explained by this missing looping. Furthermore, there are several types of ASO: the physiologic spiral anastomoses for transposing the great arteries preserving the physiological Romanesque shape of the aorta, in contrast to the Jatene procedure with the LeCompte maneuver that resembles a Gothic shaped arch. In a similar study to our current study, abnormal aortic flow profiles between two different types of ASO were reported,[18] and they showed a larger number of vortical flow features more commonly found in the aortic sinus of Valsalva in the TGA after the Jatene procedure. Furthermore, an increased non-physiological aortic helical flow in patients who underwent LeCompte technique was identified compared to those who underwent spiral technique (58% vs. 29%).[18] These results were consistent with

our current data. The Jatene procedure with LeCompte maneuver is currently the standard technique; however, it may be recommended to restore the great arteries in a spiral fashion to avoid ineffective blood-flow dynamics, from the point of aortopathy.

Aortic distensibility, WSS and EL in TGA

Disturbed flow and reciprocating shear stress have a negative impact on aortopathy and consequently promote atherogenesis and thrombogenesis, as mentioned above. Hence, an undisturbed flow is desirable for all TGA patients to optimize endothelial cell function. Distensibility of the AAO was also reported to be decreased in TGA patients, and increased carotid artery stiffness is identified by either surgical method, ASO, or atrial redirection.[19] Besides a possible genetic background, surgical transection, aortic flow reflection, manipulation of
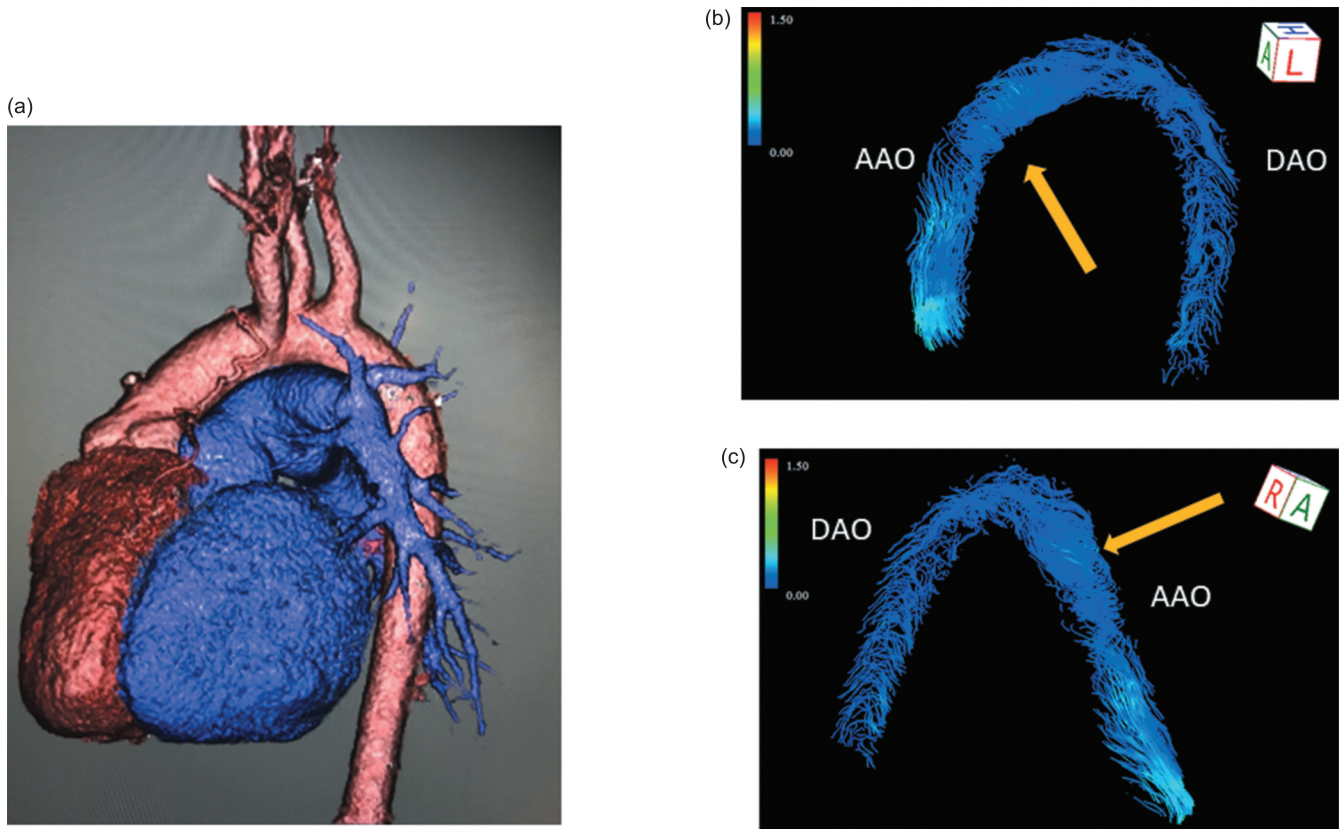
Fig. 6 4D aortic streamline image in TGA after Senning operation. A 3D image showed the aorta in a 34-year-old female after the Senning operation (**a**). Focal, non-physiological counter-clockwise flow of the AAO (orange arrow) was identified (**b** and **c**). In general, a healthy control shows clockwise laminar flow in the AAO. AAO, ascending aorta; TGA, transposition of the great arteries.

the vasa vasorum, or even denervation may impact their poor distensibility.[20–22] Overall, these negative factors can also promote aortopathy in TGA. These factors, abnormal flow dynamics, and aortopathy are the so-called "chicken or the egg causality dilemma". As shown in our current data, the larger the sinus of Valsalva, the greater the vorticity and helicity. Moreover, these negative factors may provoke larger EL of the aortic root, resulting in a great burden on the left ventricle (LV) from the ventriculo-arterial decoupling.[23] As mentioned above, EL affects the cardiac workload, which causes long-term ventricular deterioration.[6,7,23] WSS also worsens long-term vascular stiffness, and WSS caused by turbulent flow generally increases EL. In various CHDs such as tetralogy of Fallot, bicuspid aortic valve, and single ventricle after the Norwood procedure,[7,15,24] EL is reported to be elevated subsequent to abnormal aortic flow dynamics, suggesting increased cardiac workload and potential ventriculo-arterial decoupling.

In TGA patients, potential myocardial impairment compared to controls has been reported.[23] Hence, we have to carefully follow up LV function, as well as aortopathy and aortic regurgitation in these young TGA patients after the Jatene procedure. From this perspective, aortic flow profiles can be important additional determinants of fluid–vessel wall interactions. Vorticity and helicity data assessed by 4D flow MRI can be informative to disclose the secondary risk of aortopathy and to prevent the progression.

EPI 4D flow MRI

Some studies indicate that EPI 4D Flow MRI allows a reduction in scan time and better data quality than the recommended k-space segmented spoiled gradient echo sequence.[8,9] In this study, 4D flow with TFE and EPI can shorten the scan time (average scan time of approximately 4 min) and time resolution. Consequently, it enables simultaneous evaluation of the aorta, the pulmonary arteries, the venae cavae, and the pulmonary veins in complex CHD. On the other hand, some studies report that 4D flow MRI using EPI readout results not only in considerable velocity misregistration but also in spatially varying degradation of resolution, suggesting that EPI is inferior to standard GRE for 4D flow MRI.[10] This issue remains controversial.

Limitations

The number of patients enrolled in this study was small, limiting the statistical evidence. Owing to the overwhelming

Table 4 Correlations with arch angle, aortic root dilatation, and 4D flow parameters in patients after LeCompte procedure

	Arch angle		Valsalva-AAO ratio	
	R	P	R	P
R valsalva vorticity (m^2/s)	-0.70	0.037	0.72	0.029
L valsalva vorticity (m^2/s)	-0.70	0.036	0.72	0.028
R ascending aortic vorticity (m^2/s)	-0.27	0.48	0.50	0.16
L ascending aortic vorticity (m^2/s)	-0.27	0.48	0.58	0.10
R arch vorticity (m^2/s)	-0.05	0.89	0.36	0.34
L arch vorticity (m^2/s)	0.19	0.62	-0.02	0.96
R aortic isthmus vorticity (m^2/s)	-0.71	0.032	0.26	0.50
L aortic isthmus vorticity (m^2/s)	-0.72	0.028	0.17	0.75
R ascending aortic helicity (m^3/s^2)	-0.16	0.69	0.67	0.048
L ascending aortic helicity (m^3/s^2)	-0.10	0.79	0.62	0.07
R descending aortic helicity (m^3/s^2)	-0.20	0.60	0.29	0.44
L descending aortic helicity (m^3/s^2)	0.18	0.65	-0.36	0.34
WSS (Pa)	-0.18	0.64	0.40	0.29
Peak EL (mW/cm^3)	-0.46	0.21	0.69	0.04
Averaged EL (mW/cm^3)	-0.56	0.12	0.61	0.08
Valsalva- AAO ratio	-0.72	0.03	-	-

AAO, ascending aorta; EL, energy loss; L, counterclockwise; R, clockwise; WSS, wall shear stress.

prevalence of the Jatene procedure, it may, in fact, be very difficult to perform a larger retrospective comparison study; therefore, our data are still informative. Second, in our current study, seven out of nine patients in the Jatene group underwent PAB before the ASO; therefore, the influence has to be considered. However, it is difficult to enroll adult TGA patients with one-stage ASO at the present time, and further studies comparing one- and two-stage ASO are needed. Third, the temporal resolution of 4D flow MRI was limited, and the peak systolic vorticity values were most likely underestimated. We used EPI using a Philips machine; however, the maximum condition was 14 frames/cycle, which is one of the technical limitations in our present study. 4D flow MRI also provides suboptimal spatial resolution, compared to computer simulation; therefore, measurements of wall share stress can include analytical error. Furthermore, the reproducibility of 4D flow MRI is not perfect. Intra- and inter-observer agreement in our data was relatively good, but our evaluators were well-skilled, and there is a technical limitation, generally. In order to analyze these complex anatomical malformations, evaluators need to know the anatomical and surgical uniqueness because almost all cases require manual correction of the aortic wall abnormality, and the reproducibility depends on the evaluators' manual correction to some extent. Further studies are required using computational fluid dynamics.

Conclusion

A non-physiologic blood flow pattern of the aortic root was identified in TGA adults after the Jatene procedure with the LeCompte maneuver. Missing looping of the great arteries and the unique structure after the Jatene procedure may play an adjunctive role in promoting aortopathy. The evaluation of aortic flow profile using EPI 4D flow MRI may be useful for risk stratification for aortopathy in this population.

Conflicts of Interest

No disclosure in all authors.

References

1. Moe TG, Bardo DME. Long-term outcomes of the arterial switch operation for d-transposition of the great arteries. Prog Cardiovasc Dis 2018; 61:360–364.
2. Kirzner J, Pirmohamed A, Ginns J, et al. Long-term management of the arterial switch patient. Curr Cardiol Rep 2018; 20:68
3. Geiger J, Hirtler D, Bürk J, et al. Postoperative pulmonary and aortic 3D haemodynamics in patients after repair of transposition of the great arteries. Eur Radiol 2014; 24:200–208.
4. Kilner PJ, Yang GZ, Mohiaddin RH, et al. Helical and retrograde secondary flow patterns in the aortic arch studied by

three-directional magnetic resonance velocity mapping. Circ 1993; 88:2235–2247.

5. Riesenkampff E, Nordmeyer S, Al-Wakeel N, et al. Flow-sensitive four-dimensional velocity-encoded magnetic resonance imaging reveals abnormal blood flow patterns in the aorta and pulmonary trunk of patients with transposition. Cardiol Young 2014; 24:47–53.

6. Akins CW, Travis B, Yoganathan AP. Energy loss for evaluating heart valve performance. J Thorac Cardiovasc Surg 2008; 136:820–833.

7. Itatani K, Miyaji K, Qian Y, et al. Influence of surgical arch reconstruction methods on single ventricle workload in the Norwood procedure. J Thorac Cardiovasc Surg 2012; 144:130–138.

8. Viola F, Dyverfeldt P, Carlhäll CJ, et al. Data quality and optimal background correction order of respiratory-gated k-Space Segmented Spoiled Gradient Echo (SGRE) and Echo Planar Imaging (EPI)-Based 4D flow MRI. J Magn Reson Imaging 2020; 51:885–896.

9. Garg P, Westenberg JJM, van den Boogaard PJ, et al. Comparison of fast acquisition strategies in whole-heart four-dimensional flow cardiac MR: Two-center, 1.5 Tesla, phantom and in vivo validation study. J Magn Reson Imaging 2018; 47:272–281.

10. Dillinger H, Walheim J, Kozerke S. On the limitations of echo planar 4D flow MRI. Magn Reson Med 2020; 84:1806–1816.

11. Schäfer M, Barker AJ, Kheyfets V, et al. Helicity and vorticity of pulmonary arterial flow in patients with pulmonary hypertension: quantitative analysis of flow formations. J Am Heart Assoc 2017; 6:e007010.

12. Hasegawa T, Oshima Y, Maruo A, et al. Aortic arch geometry after the Norwood procedure: The value of arch angle augmentation. J Thorac Cardiovasc Surg 2015; 150:358–366.

13. Lalezari S, Mahtab EA, Bartelings MM, et al. The outflow tract in transposition of the great arteries: an anatomic and morphologic study. Ann Thorac Surg 2009; 88:1300–1305.

14. Warnes CA. Transposition of the great arteries. Circ 2006; 114:2699–2709.

15. Garcia J, Barker AJ, Collins JD, et al. Volumetric quantification of absolute local normalized helicity in patients with bicuspid aortic valve and aortic dilatation. Magn Reson Med 2017; 78:689–701.

16. Geiger J, Hirtler D, Gottfried K, et al. Longitudinal evaluation of aortic hemodynamics in Marfan syndrome: new insights from a 4D flow cardiovascular magnetic resonance multi-year follow-up study. J Cardiovasc Magn Reson 2017; 19:33.

17. Ding Z, Fan Y, Deng X, et al. Effect of swirling flow on the uptakes of native and oxidized LDLs in a straight segment of the rabbit thoracic aorta. Exp Biol Med (Maywood) 2010; 235:506–513.

18. Rickers C, Kheradvar A, Sievers HH, et al. Is the Lecompte technique the last word on transposition of the great arteries repair for all patients? A magnetic resonance imaging study including a spiral technique two decades postoperatively. Interact Cardiovasc Thorac Surg 2016; 22:817–825.

19. Voges I, Jerosch-Herold M, Hedderich J, et al. Implications of early aortic stiffening in patients with transposition of the great arteries after arterial switch operation. Circ Cardiovasc Imaging 2013; 6:245–253.

20. Lalezari S, Hazekamp MG, Bartelings MM, et al. Pulmonary artery remodeling in transposition of the great arteries: relevance for neoaortic root dilatation. J Thorac Cardiovasc Surg 2003; 126:1053–1060.

21. Parke WW. The vasa vasorum of the ascending aorta and pulmonary trunk and their coronary-extracardiac relationships. Am Heart J 1970; 80:802–810.

22. Stefanadis CI, Karayannacos PE, Boudoulas HK, et al. Medial necrosis and acute alterations in aortic distensibility following removal of the vasa vasorum of canine ascending aorta. Cardiovasc Res 1993; 27:951–956.

23. Biglino G, Ntsinjana H, Plymen C, et al. Ventriculovascular interactions late after atrial and arterial repair of transposition of the great arteries. J Thorac Cardiovasc Surg 2014; 148:2627–2633.

24. Schäfer M, Barker AJ, Jaggers J, et al. Abnormal aortic flow conduction is associated with increased viscous energy loss in patients with repaired tetralogy of Fallot. Eur J Cardiothorac Surg 2020; 57:588–595.